View metadata, citation and similar papers at core.ac.uk brought to you by CORE
provided by Electronic Sumy State University Institutional Repository

PROCEEDINGS OF THE INTERNATIONAL CONFERENCE
NANOMATERIALS: APPLICATIONS AND PROPERTIES
Vol. **3** No 1, 01PCSI10(4pp) (2014)

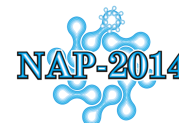

X-Ray Diffraction Characterization of Nanoscale Strains and Defects in Yttrium Iron Garnet Films Implanted with Fluorine Ions

S.I. Olikhovskii[1,*], O.S. Skakunova[1], V.B. Molodkin[1], V.V. Lizunov[1], Ye.M. Kyslovs'kyy[1], T.P.Vladimirova[1], O.V. Reshetnyk[1], V.M. Pylypiv[2], V.O. Kotsyubynsky[2], B.K. Ostafiychuk[2], I.P. Yaremiy[2], O.Z.Garpul'[2]

[1] *G.V. Kurdyumov Institute for Metal Physics of NASU, 36, Vernadsky Blvd., 03680 Kyiv, Ukraine*
[2] *V. Stefanyk Precarphatian National University, 57, Shevchenko Str., 76025 Ivano-Frankivsk, Ukraine*

(Received 14 July 2014; published online 29 August 2014)

The theoretical diffraction model for a crystalline multilayer system with inhomogeneous strain profile and randomly distributed defects has been created by using the statistical dynamical theory of X-ray diffraction in imperfect crystals. The dynamical scattering peculiarities in both coherent and diffuse scattering intensities have been taken into account for all the layers of the system by using derived recurrence relations between coherent scattering amplitudes.

The investigated yttrium-iron garnet films grown on gadolinium-gallium garnet substrate were implanted with different doses of 90 keV F^+ ions. The rocking curves measured from the as-grown and implanted samples have been treated by using the proposed theoretical model. This model has allowed for the reliable self-consistent determination of strain profile parameters and structural defect characteristics in both implanted film and substrate of the investigated samples.

Keywords: X-Ray diffraction theory, Yttrium iron garnet, Film, Ion implantation, Strain, Defects.

PACS numbers: 61.05.Cc, 61.05.Cp, 61.72.Dd, 61.72.jd, 61.72.Nn, 61.72.Qq, 61.80.Jh, 61.82.Ms

1. INTRODUCTION

Epitaxial single-crystalline yttrium iron garnet (YIG) $Y_3Fe_5O_{12}$ films grown on gadolinium gallium garnet (GGG) $Gd_3Ga_5O_{12}$ substrate are widely used in various scientific research and technical application fields. In particular, YIG films are used as sensors in magnetometers for the visual observation of the spatial distribution of inhomogeneous magnetic fields, in energy-independent magnetic memory devices, in magnetic microelectronics and integral magneto-optics, etc. (see, e.g., Refs. [1-3]).

Ion implantation is the effective technique for purposeful modifying the crystalline structure of subsurface layers in such films and, thus, for changing their physical properties, in particular, magnetic, optical, and magneto-optical ones [4-6]. However, despite the numerous experimental and theoretical investigations of ion-implanted garnets (see also Refs. [7-10]), some questions remain insufficiently elucidated, in particular, concerning processes of the formation of primary and secondary defects in YIG films after ion implantation and their relation with parameters of crystalline microstructure.

To characterize structural defects and strains in the modified crystal layers, the X-ray diffraction methods are most widely used. Efficiency of application of these methods is dependent to large extent on the availability of the analytical formulas which give the adequate description of measured diffraction intensity distributions. In particular, there exist various theoretical models to describe the rocking curves (RCs) which are measured from imperfect crystalline structures with inhomogeneous strain profiles [7-9, 11, 12] and additional structure imperfections [13, 14-16].

The aim of the present work consists in the demonstration of characterization possibilities of the generalized statistical dynamical theory of X-ray diffraction, which has been extended to the case of imperfect crystals with randomly distributed defects and inhomogeneous strain profiles caused by ion implantation [16]. The proposed diffraction model will be applied to characterize nanometer-sized defects and strains in the epitaxial YIG films grown on GGG substrate, which were implanted with 90 keV F^+ ions at different doses, by using the RCs measured by the high-resolution double-crystal X-ray diffractometer (DCD).

2. REFLECTIVITY OF INHOMOGENEOUS STRUCTURES WITH DEFECTS

The multilayer system which consists of GGG substrate covered on both sides by single-crystalline YIG films is characterized from the structural point of view by the presence of growth defects in the volumes of both substrate and films as well as inhomogeneous strain in subsurface and transition layers. Ion implantation of this system results in the appearance of primary and secondary radiation defects which cause the additional strain in subsurface layers with constant and fluctuation components.

To describe analytically X-ray diffraction in such a system we can subdivide it into M+1 laminae and consider as a multilayer crystal system with constant average strain in each lamina. Then, we can make use of the recurrence relations between coherent components of amplitude reflection coefficients of adjacent layers in

[*] olikhovsky@meta.ua

 © 2014 Sumy State University

the two-wave approximation for Bragg diffraction geometry [15, 16]:

$$R_j = \frac{r_j + R_{j-1}\left(t_j^2 e_j^{-1} - r_j^2 \zeta_j^{-1}\right)}{1 - \zeta_j^{-1} r_j R_{j-1}}, \tag{1}$$

where r_j and t_j are the dynamical amplitude reflection and transmission coefficients of j th layer with randomly distributed defects, respectively, e_j is the phase factor, the constant $\zeta_j \sim 1$, and the subscript $j = 0, 1, \ldots, M$ denotes the relation of corresponding quantity to jth layer .

The coherent component of RC for the multilayered crystal system which consists of M+1 layers with randomly distributed defects can be represented as follows:

$$R_{\mathrm{coh}}(\Delta\theta) = \left| R_M(\Delta\theta) \right|^2, \tag{2}$$

where $\Delta\theta$ is an angular deviation of the investigated sample from an exact Bragg position, and the amplitude reflectivity of upper Mth layer $R_M(\Delta\theta)$ can be determined by using the recurrence relation (1). The starting value in this relation, the dynamical amplitude reflection coefficient of 0th layer corresponding to the thick substrate with defects, is calculated as follows:

$$R_0(\Delta\theta) = \zeta^{1/2}\left[y_0 - \mathrm{sgn}(y_{0\mathrm{r}} y_{0\mathrm{i}}) \sqrt{y_0^2 - 1} \right], \tag{3}$$

where quantities $y_{0\mathrm{r}} = \mathrm{Re}\, y_0$ and $y_{0\mathrm{i}} = \mathrm{Im}\, y_0$ denote real and imaginary parts of the normalized angular deviation of the substrate y_0 from an exact Bragg reflection position.

The diffuse component of the RC for multilayered system, which is measured by DCD with widely open detector window and represents the differential diffuse scattering (DS) intensity integrated over exit angles, can be written as the sum of diffuse reflectivities of each layer with proper extinction and absorption factors [7]:

$$R_{\mathrm{diff}}(\Delta\theta) = \sum_{j=0}^{M} F_{\mathrm{abs}}^j F_{\mathrm{ext}}^j R_{\mathrm{diff}}^j, \tag{4}$$

where F_{ext}^j and F_{abs}^j are extinction and absorption factors, respectively.

Diffuse reflectivities of thick substrate (j =0) and thin layers ($j = \overline{1, M}$) in Eq. (4) are calculated as follows:

$$R_{\mathrm{diff}}^j = \frac{\mu_{\mathrm{ds}}^j(\Delta\theta) d_j}{\gamma_0}, \quad R_{\mathrm{diff}}^0 = \frac{\mu_{\mathrm{ds}}^0(\Delta\theta)}{(1+b)\mu_0^0}, \tag{5}$$

where μ_0^j and μ_{ds}^j are photoelectric absorption coefficient and absorption coefficient due to DS in jth layer, respectively, d_j is the thickness of jth layer, γ_0 is the direction cosine of the incident X-ray, b is the diffraction asymmetry factor.

It should be remarked here that the absorption coefficients due to DS from several types of randomly distributed defects without correlations between them are summarized, similarly to exponents of corresponding static Debye-Waller factors.

3. EXPERIMENTAL

Epitaxial single-crystalline YIG films with 5.33 μm thickness were grown by Czochralsky method on both sides of 500 μm thick GGG substrates with [111] growth axis. The samples after lapping were polished mechanically, chemo-dynamically, and chemically. The investigated samples have been implanted with F^+ ions at the energy of 90 keV and with doses $D = 1 \times 10^{13}$, 6×10^{13}, and 2×10^{14} cm^{-2}.

Experimental RCs of the implanted samples were measured by using the high-resolution four-circle X-ray DCD with Cu tube (25 kV × 25 mA) and two flat Ge (333) monochromators in the antiparallel setting. The symmetric (444) (see Fig. 1) and (888) reflections were used at the samples under investigation.

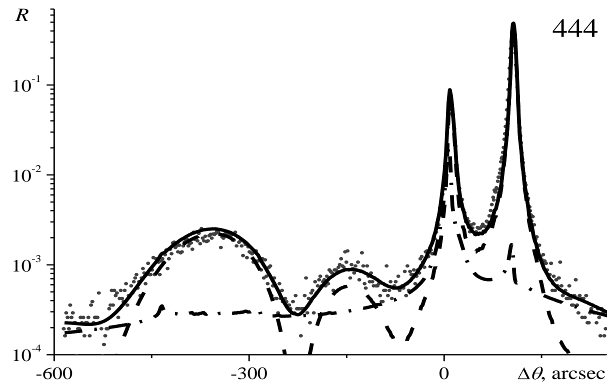

Fig. 1 – Measured and calculated (solid line) RCs for 444 reflection of $CuK_{\alpha 1}$ radiation from YIG/GGG film system implanted with F^+ ions (E = 90 keV) at doses $D = 6 \times 10^{12}$ cm^2. Coherent and diffuse RC components are shown by dashed and dot-dashed lines, respectively

4. THE STRUCTURE MODEL OF THE IMPLANTED YIG/GGG SYSTEM

For realization of quantitative diagnostics of imperfect structure of a single-crystalline inhomogeneous system by X-ray diffraction methods it is necessary to use the adequate structural model. In garnet crystals, there always are present various point defects and growth microdefects, including new phase particles and dislocation loops (see, e.g., Ref. [18]. In garnet films, additionally to fluctuation strain fields from randomly distributed defects, the smooth inhomogeneous strain fields are created in transitional layers between film and substrate due to lattice mismatch [9].

After ion implantation, the subsurface layer of a film is additionally saturated with primary and secondary radiation defects, which are distributed inhomogeneously in depth and cause the corresponding «in average» inhomogeneous strain. Separate isolated amorphous clusters that arise at bombardment of garnet films with light ions of intermediate energies are relatively stable [5, 6].

Thus, in the model of defect structure of the implanted epitaxial single-crystalline system of YIG films grown on GGG substrate the presence of two types of microdefects, namely, spherical clusters and circular prismatic dislocation loops was supposed. The influence of point defects (antisite defects and anion vacancies) and thermal DS was taken into account as well [18]. The film system in whole was considered as a multilayer system in each layer of which the strain was consisted of average and fluctuating components. The change of YIG and GGG cubic lattice constants due to point defects was calculated according to empiric analytical expression through concentrations of these defects and effective radii of cations [18].

When fitting theoretical RCs, the depth profiles of the strain caused by implantation were calculate through concentrations of the amorphous clusters formed by displaced matrix atoms in consequence of energy losses of the implanted ions [6]. The existence of two channels of energy losses for the implanted light ions was taken into account, namely, through excitation of electronic subsystem and through elastic nuclear collisions [10]. For electronic and nuclear channels channel this depth profile was set as a decreasing tail of Gaussian and asymmetric Gaussian, respectively.

Such characteristics of clusters in implanted layer as radius and strain at the boundary with crystal matrix were supposed to be equal for both channels. Resulting strain profile in implanted layer was calculated as the sum of depth-depended strain profiles created by the two distributions of cluster concentrations along the normal to crystal surface.

The depth profile of the so-called amorphization factor was described in our diffraction model by only the static Debye-Waller factor, exponent of which was calculated through characteristics of clusters in implanted layer as well. Additionally, the attenuation of coherent component of diffraction intensity from the implanted layer was described by the coefficient of absorption due to DS μ_{ds}^{j}, which was calculated similarly through characteristics of clusters in implanted layer.

Thus, the chosen model of imperfect structure of the implanted YIG film on GGG substrate provides physically clear connection between defect characteristics and structurally sensitive diffraction parameters. Also, the self-consistent character of calculation of these parameters should be emphasized, what complements the self-consistency between coherent and diffuse components of diffraction intensity in the present diffraction model.

5. TREATMENT AND DISCUSSION

The RC measured from a multilayer system like the implanted YIG film on GGG substrate is formed by a superposition of angular distributions of coherent and DS intensities from substrate, film, and implanted layer. Such superposition complicates the analysis of the RC for the assessment of strain and amorphization parameters in the implanted layer since the numerous additional fit parameters arise, which characterize defect structure of film and substrate.

On the other hand, the account for influence of DS effects from dislocation loops and clusters in film and substrate on the form of diffraction peaks and tails has allowed for both the determination of as-grown defect characteristics (see Table 1) and correct description of X-ray intensity diffracted from the implanted layer. Also, such account has provided the possibility to avoid systematical errors when determining strain and defect characteristics in this layer.

Table 1 – Characteristics of circular dislocation loops and spherical clusters in YIG film and GGG substrate

Defects	Characteristics	GGG substrate		YIG film
Circular dislocation loops	Radius, nm	90	5	5
	Density, cm^{-3}	$1{,}2\times10^{12}$	1×10^{15}	1×10^{15}
Spherical clusters	Radius, nm	8		10
	Density, cm^{-3}	1×10^{14}		1×10^{14}

At modeling the strain distribution, the implanted layer was subdivided into 2 nm thick laminae, whereas the rest of film and substrate volume was subdivided into layers with thicknesses of order of few hundreds of nanometers. It was supposed that as a result of electronic and nuclear energy losses of implanted ions the spherical amorphous clusters were formed in the implanted layer. Their radii have been determined to be approximately 1.7 nm at the value of volume strain between cluster and crystal matrix $\varepsilon = 0.03$. The corresponding cluster concentrations found at various implantation doses are given in Table 2.

Table 2 – Maximal values of cluster concentrations and strain profiles in YIG film implanted with F^{+} ions (E = 90 keV) at various implantation doses

D, cm^{-2}	1×10^{13}	6×10^{13}	2×10^{14}
$n_C^{nucl,max}$, cm^{-3}	1.1×10^{19}	6×10^{19}	2×10^{20}
$n_C^{el,max}$, cm^{-3}	1.10×10^{19}	6.00×10^{19}	2.00×10^{20}
$\varepsilon_{\perp}^{nucl,max}$, %	0.10	0.54	1.79
$\varepsilon_{\perp}^{el,max}$, %	0.04	0.22	0.73

It should be emphasized that values of the parameters that define the form of strain profile have been determined to be the same for all the implantation doses and both reflections measured (see Figs. 2 and 3).

Thus, the complete set of defect characteristics and strain parameters of the implanted layers in YIG films on GGG substrates has been determined by the fully dynamical self-consistent treatment of diffraction profiles from the investigated samples simultaneously for two reflections. The self-consistentcy of the description of coherent and diffuse components of diffraction patterns has been achieved due to the fully dynamical interpretation from such systems becomes possible with, which are connected analytically with strain and defect characteristics.

Additionally, the strain distribution in the transition layer between film and substrate has been determined, which thickness approaches some hundreds of nanometers (see Fig. 3).

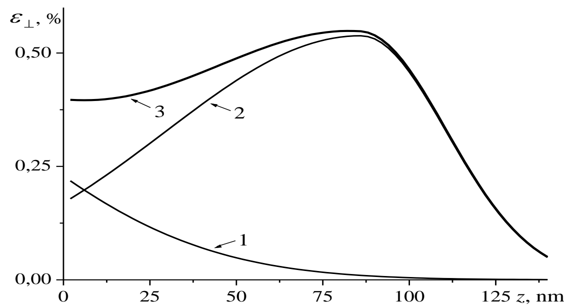

Fig. 2 – Strain profiles in implanted layer of YIG film, which are caused by electronic (1), nuclear (2), and total (3) energy loses of implanted F^+ ions (E = 90 keV, D = 6×10^{13} cm^2)

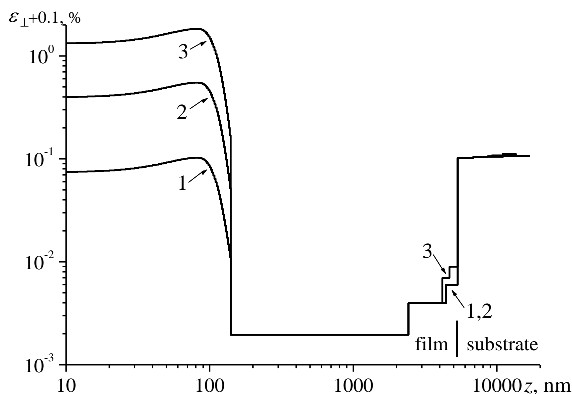

Fig. 3 – Strain profiles in YIG/GGG film system implanted with F^+ ions (E = 90 keV) at doses D = 1×10^{13} (1), 6×10^{13} (2), and 2×10^{14} cm^2 (3), respectively.

6. RESUME AND CONCLUSIONS

The theoretical diffraction model, based on the generalized statistical dynamical theory of X-ray scattering in imperfect crystals, has been proposed to describe RCs from imperfect film structures with randomly distributed defects and the inhomogeneous strain profile caused by ion implantation. The dynamical character of both coherent and diffuse components has been taken into account by means of recurrence relations between coherent scattering amplitudes of adjacent crystal layers. Thus, the fully dynamical interpretation of diffraction patterns from such systems becomes possible with self-consistent description of the coherent and diffuse components, which are connected analytically with strain and defect characteristics.

The proposed diffraction model has been applied to characterize defects and strains in the epitaxial YIG films grown on GGG substrate, which were implanted with of 90 keV F^+ ions at various doses. Simultaneous treatment of the RCs measured by the high-resolution DCD with widely open detector window for two reflections has provided the set of the parameters, which characterize both strain and defects in both implanted layer and YIG film on GGG substrate.

AKNOWLEDGEMENTS

This research was supported by the National Academy of Sciences of Ukraine under contract No. 3.6.3.13-7/14-D.

REFERENCES

1. A.K. Zvezdin, V.A. Kotov, *Modern Magnetooptics and Magnetooptical Materials* (New York: Taylor & Francis Group: 1997).
2. T. Aichele, A. Lorenz, R. Hergt, P. Görnert, *Cryst. Res. Technol.* **38**, 575 (2003).
3. T. Wehlus, T. Körner, S. Leitenmeier, A. Heinrich, B. Stritzker, *phys. status solidi a* **208**, 252 (2011).
4. V.S. Speriosu, C.H. Wilts, *J. Appl. Phys.* **54**, 3325 (1983).
5. B. Lagomarsino, A. Tucciarone, *Thin Solid Films* **114**, 45 (1984).
6. P. Gerard, *Nucl. Instrum. Meth. Phys. Res. B* **19–20**, 843 (1987),
7. V. S. Speriosu, *J. Appl. Phys.* **52**, 6094 (1981).
8. C. R. Wie, T. A. Tombrello, T. Vreeland, Jr., *J. Appl. Phys.* **59**, 3743 (1986).
9. M. Dimer, E. Gerdau, R. Rüffer, H. D. Rüter, W. Sturhahn, *J. Appl. Phys.* **79**, 9090 (1996).
10. B.K. Ostafiychuk, V.D. Fedoriv, I.P. Yaremiy, O.Z., Garpul, V.V. Kurovets, I.C. Yaremiy, *phys. status solidi a* **208**, 2108 (2011).
11. R.N., Kyutt, P.V. Petrashen, L.M. Sorokin, *phys. status solidi a* **60**, 381 (1980).
12. Yu.N. Belyaev, A.V. Kolpakov, *phys. status solidi a* **76**, 641 (1983).
13. V.I. Punegov, *phys. status solidi a* **136**, 9 (1993).
14. P.K. Shreeman, R.J. Matyi, *J. Appl. Cryst.* **43**, 550 (2010).
15. V.B. Molodkin, S.I. Olikhovskii, Ye.M. Kyslovskyy, I.M. Fodchuk, E.S. Skakunova, E.V. Pervak, V.V. Molodkin, *phys. status solidi a* **204**, 2606 (2007).
16. V.M. Pylypiv, S.I. Olikhovskii, T.P. Vladimirova, O.S. Skakunova, V.B. Molodkin, B.K. Ostafiychuk, Ye.M. Kyslovskyy, O.V. Reshetnyk, S.V. Lizunova, O.Z. Garpul', *Metallofiz. Noveishie Tekhnol.* **33**, 1145 (2011).
17. V.B. Molodkin, S.I. Olikhovskii, E.N. Kislovskii, TP. Vladimirova, E.S. Skakunova, R.F. Seredenko, B.V. Sheludchenko, *Phys. Rev. B* **78**, 224109 (2008).
18. V.M. Pylypiv, T.P. Vladimirova, I.M. Fodchuk, B.K. Ostafiychuk, Ye.M. Kyslovskyy, V.B. Molodkin, S.I. Olikhovskii, O.V. Reshetnyk, O.S. Skakunova, V.V. Lizunov, O.Z. Garpul', *phys. status solidi a* **208**, 2558 (2011).